

LY α ABSORBERS DO/NOT CO-ROTATE WITH GALAXY DISKS

DAVID M. FRENCH, BART P. WAKKER

Department of Astronomy, University of Wisconsin, Madison, WI 53706, USA

Draft version October 18, 2017

ABSTRACT

We present results of a study comparing the relative velocity of Ly α absorbers to the rotation direction and velocity of nearby galaxy disks. We find...

Subject headings: galaxies:intergalactic medium, galaxies:evolution, galaxies:halos, quasars: absorption lines

1. INTRODUCTION

Galaxy rotation curves have been observed to extend at constant velocity out to... (cite...). It becomes increasingly difficult to measure gas rotation much farther from this however, as the... Within this region the galaxy disks transition into circumgalactic medium (CGM), and eventually the CGM merges with the intergalactic medium (IGM). At what point, however, does the surrounding medium cease to circulate with the galaxy? Stewart et al. (2011) suggests through (HYDRO?) simulations that the bulk CGM kinematics out to (WHAT DISTANCE) may circulate, and that absorption in intervening QSO sightlines should be able to accurately capture this rotation signature.

2. DATA AND ANALYSIS

2.1. SALT Data

Our sample 14 contains 14 galaxies observed with the Southern African Large Telescope (SALT) Robert Stobie Spectrograph (RSS) in longslit mode. These 14 were selected from a larger pool of 48 submitted targets by the SALT observing queue. These 48 possible targets were chosen for their proximity to background QSOs whose spectra contained promising Ly α lines. Finally, we only included galaxies with $z \leq 0.33$ ($cz \leq 10,000$ km s⁻¹), angular sizes less than 6' to ensure easy sky subtraction, and surface brightnesses sufficient to keep exposure times below 1300s. Table 2 summarizes these observations.

All SALT galaxy spectra were reduced and extracted using the standard PySALT reduction package (CITATION), which includes procedures to prepare the data, correct for gain, cross-talk, bias, and overscan, and finally mosaic the images from different extensions. Next, we rectify the images with wavelength solutions found via Ne and Ar arc lamp spectra line identification. Finally, we perform a basic sky subtraction using an off-sky portion of the image, and extract 5-10 pixel wide 1-D strips from the reduced 2-D spectrum.

For each 1-D spectrum, we identify the H α emission or Ca H&K absorption lines and perform a non-linear least-squares Voigt profile fit using the Python package LMFIT¹. The line centroid and 1σ standard errors are returned, and these fits are then shifted to rest-velocity based on the galaxy systemic redshift and heliocentric velocity corrections are calculated with the IRAF rvcorrect

procedure. The final rotation velocity is calculated by then applying the inclination correction, $v_{rot} = v/\sin(i)$. Final errors are calculated as

$$\sigma^2 = \left(\frac{\partial v_{rot}}{\partial \lambda_{obs}}\right)^2 (\Delta \lambda_{obs})^2 + \left(\frac{\partial v_{rot}}{\partial v_{sys}}\right)^2 (\Delta v_{sys})^2 + \left(\frac{\partial v_{rot}}{\partial i}\right)^2 (\Delta i)^2, \quad (1)$$

where $\Delta \lambda_{obs}$, Δv_{sys} , and Δi are the errors in observed line center, galaxy redshift, and inclination, respectively. The final physical scale is calculated using the SALT image scale of 0.1267 arcsec/pixel, multiplied by the 4-pixel spatial binning, and converted to physical units using a redshift-independent distance if available, and a Hubble flow estimate if not. We adopt a Hubble constant of $H_0 = 71$ km s⁻¹Mpc⁻¹ throughout.

Finally, we calculate our approaching and receding velocities via a weighted mean of the outer 1/2 of each rotation curve, with errors calculated as weighted standard errors in the mean. Our final redshifts are calculated by forcing symmetric rotation, such that the outer 1/2 average velocity for each side matches. See Figure ?? for an example.

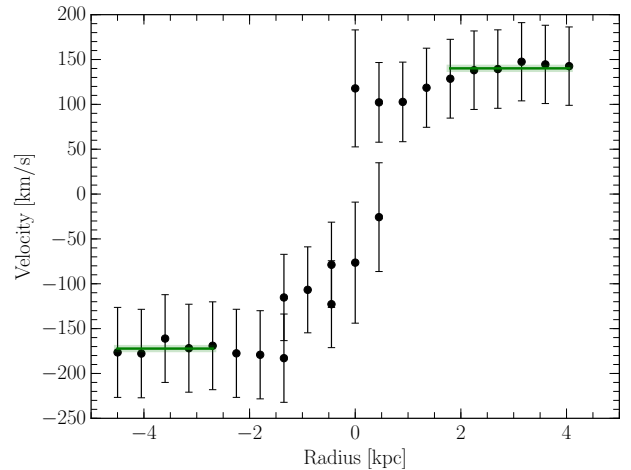


Figure 1. Rotation curve of NGC3633. The solid green line indicates the weighted mean velocity over the corresponding x-axis region, and the shaded green indicates the 1σ error in the mean.

¹ <http://cars9.uchicago.edu/software/python/lmfit/contents.html>

Target	R.A.		Dec.		z		Program	Grating	Obs ID	Obs Date	T_{exp}^* [ks]	S/N* [1238]
(1)	(2)		(3)		(4)		(5)	(6)	(7)	(8)	(9)	(10)
1H0717+714	7.0	21.0 53.3	71.0	20.0 36.0	0.5003		12025	G130M	LBG812	11-12-27	6.0	37

Table 1

COS targets in this sample. *Total exposure time and S/N ratio is given for multi-orbit exposures.

Galaxy	R.A.		Dec.		cz (km s ⁻¹)	Type	Grating	LOS Velocity (km s ⁻¹)	Absolute Velocity (km s ⁻¹)	Obs Date	T_{exp} (ks)	S/N (6562.8)
(1)	(2)		(3)		(4)	(5)	(6)	(7)	(8)	(9)	(10)	(11)
NGC4536	12 34	27.05	+02 11	17.3	1808 ± 1	SAB(rc)bc	PG2300	-107 ± 8.5 145 ± 31.8	-113 ± 9.2 113 ± 34.3	05 11 2016	1300	not sure
NGC3633	11 20	26.22	+03 35	08.2	2600 ± 2	SAa	PG2300	-160 ± 5.7 139 ± 3.3	-169 ± 6.0 146 ± 3.5	05 11 2016	1200	not sure
NGC5786	14 58	56.26	-42 00	48.1	2998 ± 5	(R')SB(s)bc	PG2300	not sure ±	not sure ±	05 11 2016	250	not sure
NGC5364	13 56	12.00	+05 00	52.1	1241 ± 4	SA(rs)bc pec	PG2300	not sure	not sure	05 11 2016	700	not sure

Table 2

SALT targeted galaxies. Columns are as follows: 1) the galaxy name, 2), 3) R.A., Dec. in J2000, 4) galaxy systemic velocity, 5) morphological type (RC3), 6) RSS grating used, 7) approaching side velocity, 8) receding side velocity, 9) observation date, 10) exposure time, and 11) S/N of the H α or Ca H&K lines.

2.1.1. NGC4536

The data on the receding side of NGC4536 is very messy, and may include contamination from background sources.

2.1.2. NGC3633

Several locations show two velocities for emission. We have combined these into a single velocity measurement via a weighted average. We measure a redshift for this galaxy of $cz = 2597.6 \pm 2.4$ km s⁻¹.

We measure a line-of-sight rotation velocity for NGC3633 of $v_{rot} = 139 \pm 3.3, -160 \pm 5.7$, km s⁻¹.

2.1.3. NGC5364

2.1.4. NGC5786

2.2. Ancillary Data

2.3. Galaxy Data

2.4. Spectra

3. RESULTS

To facilitate this decision, we calculate the likelihood, \mathcal{L} , of every possible galaxy-absorber pairing as follows:

$$\mathcal{L} = A e^{-\left(\frac{\rho}{R_{eff}}\right)^2} e^{-\left(\frac{\Delta v}{200}\right)^2}. \quad (2)$$

Here ρ is the physical impact parameter, Δv the velocity

difference between the absorber and the galaxy ($\Delta v = v_{galaxy} - v_{absorber}$), and A is a factor included to increase the likelihood in the case that $\rho \leq R_{eff}$ (in which case $A = 2$, otherwise $A = 1$).

4. SUMMARY

• First result

This research has made use of the NASA/IPAC Extragalactic Database (NED) which is operated by the Jet Propulsion Laboratory, California Institute of Technology, under contract with the National Aeronautics and Space Administration. Based on observations with the NASA/ESA *Hubble Space Telescope*, obtained at the Space Telescope Science Institute (STScI), which is operated by the Association of Universities for Research in Astronomy, Inc., under NASA contract NAS 5-26555. **SALT ACKNOWLEDGEMENT.** Spectra were retrieved from the Barbara A. Mikulski Archive for Space Telescopes (MAST) at STScI. Over the course of this study, D.M.F. and B.P.W. were supported by grant AST-1108913, awarded by the US National Science Foundation, and by NASA grants *HST*-AR-12842.01-A, *HST*-AR-13893.01-A, and *HST*-GO-14240 (STScI).

HST (COS)

<i>Target</i>	<i>Galaxy</i>	R_{vir} (kpc)	v_{galaxy} (km s ⁻¹)	<i>Inc.</i> (deg)	<i>Az.</i> [deg]	ρ (kpc)	$v_{Ly\alpha}$ (km s ⁻¹)	$W_{Ly\alpha}$ (km s ⁻¹)	Δv (km s ⁻¹)	\mathcal{L}
(1)	(2)	(3)	(4)	(5)	(6)	(7)	(8)	(9)	(10)	(11)
1H0717+714	UGC03804	173	2887	55	7	207	2870	343±6	17	0.24

Table 3

All associated systems. The largest \mathcal{L} value is given, with a (*) indicating that this corresponds to $\mathcal{L}_{d^{1.5}}$, otherwise the quoted \mathcal{L} was computed with R_{vir} .

Statistic	Blueshifted Absorbers	Redshifted Absorbers
Number	22	26
Mean EW [mÅ]	329 ± 52	245 ± 34

Table 4

Average properties of the associated galaxy sample split into red and blue-shifted bins based on Δv .